PERIODICA POLYTECHNICA SER. CIV. ENG. VOL. 44, NO. 2, PP. 135–150 (2000)

CHLORIDE ION BINDING CAPACITY OF TETRACALCIUM ALUMINOFERRITE

Jolán CSIZMADIA*, György BALÁZS*[1] and Ferenc D. TAMÁS**

*Department of Building Materials and Engineering Geology
Technical University of Budapest
H–1521 Budapest, Hungary
**Department of Silicate- and Materials Engineering
University of Veszprém
Veszprém, Hungary
[1]Corresponding author
Tel. +36-1-463 2226
Fax +36-1-463 3450
E-mail address: balazs@vasbeton.vbt.bme.hu

Received: March 5, 2000

Abstract

The hydration of aluminoferrites and their mixture with gypsum (up to 10/5 ratio) was investigated as well as their chloride binding capacity (after immersion in 10% NaCl solution) by thermal tests (DTG and TGA) and X-ray diffraction. In this first part, C_4AF has been investigated, to be followed by C_6AF_2 and C_6A_2F in the second part. Hydration products of C_4AF are similar to that of C_3A, but amorphous AH_3 and/or FH_3 are formed, and the transformation of metastable (hexagonal hydrates) to the stable (hydrogarnet) phase is slower. In case of C_4AF + gypsum mixtures, monosulfate was found prior to the total exhaustion of gypsum. After salt treatment, iron-containing Friedel's salt or Kuzel's salt was found. Characteristics of DTG peaks are described and interpreted.

Keywords: calcium aluminoferrite; chloride; thermal analysis; X-ray diffraction.

1. Introduction

This paper deals with the chloride binding capacity of calcium aluminoferrites, especially in the presence of gypsum, a constant ingredient of portland cement. A former research shows that aluminoferrites react with chloride only after the exhaustion of available sulfates, to give a complex aluminoferrite sulfate hydrate (AFm or AFt)[2], if the chloride compound is added jointly with mixing water. From this a question arises: can the anion of the AFm or AFt in hardened cement paste be exchanged by chloride during deicing salt treatment? This is the more important question, as high-iron cements are frequently used because of their high sulfate and seawater resistance.

[2]Conventional cement chemical nomenclature is used in most cases. The following symbols are used:
$C = CaO$, $S = SiO_2$, $A = Al_2O_3$, $F = Fe_2O_3$, $H = H_2O$, $\hat{S} = SO_3$, $\hat{C} = CO_2$. AFm and AFt mean calcium alumino-ferrite monosubstituted, and calcium alumino-ferrite trisubstituted, resp.

Hydration products of aluminoferrite phases are similar to those of tricalcium aluminate: in the presence of gypsum, AFm and/or AFt phases ('monosulfate' and ettringite, resp.) are formed, with the difference that in tricalcium aluminate the calcium to sesquioxide ratio is 3, while in the aluminoferrites this ratio is 2; this means that besides AFm and AFt, aluminum and/or iron hydroxides are formed, too. As most of these hydroxides are amorphous, XRD cannot be used for identification; alternative methods, as e.g. Mössbauer spectroscopy must be used instead. Reaction rates are, however, different: the hydration of aluminoferrites is slower, and this rate is further decreased by the presence of calcium hydroxide, gypsum or both. The first hydration product is ettringite, but this is later transformed to monosulfate, after the exhaustion of the available gypsum [1], [2].

Several mechanisms exist of chloride binding during cement hydration: chloride may be bonded in the C-S-H gel, as a complex calcium oxychloride, Friedel's salt (a chloride-containing AFm phase, $C_3A \cdot CaCl_2 \cdot H_{10}$), or its high-iron analogue, $C_3F \cdot CaCl_2 \cdot H_{10}$ may form too. In sulfate resistant portland cement, if a high amount of aluminum is bonded as calcium aluminoferrite, rather than tricalcium aluminate, the main product is this latter analogue, [3].

Friedel's salt is stable in basic solutions (pH $>$ 12) but it is de-stabilised at lower pH values (e.g. by carbonation). If carbonation degree is low, other phases of hydrated cement (e.g.lime hydrate or C-S-H) gel buffer pH value, so Friedel's salt, and possibly other AFm phases locally survive [4]. Other factors, which cause a decrease of pH, as the presence of acid additives or aggregates (silica fume and similar) affect the stability of Friedel's salt and, as a consequence, the resistance of cement against de-icing salt treatment.

The stability of Friedel's salt in concrete structural elements is somewhat more complicated. When concrete slabs are subjected to atmospheric carbonation and chloride attack simultaneously, then the surface carbonation (in the top 5 mm layer) is so severe, that not only Friedel's salt, but also ettringite do not exist any more [5].

Chloride binding of cement is influenced by other factors, too, e.g. alkali content appears to have an inhibiting effect on the chloride binding capacity. This fact, however, is overshadowed by a conjoint strong elevation of the OH^--ion concentration in the pore solution, causing a net lowering of the Cl^-/OH^- ratio, which in turn reduces corrosion risk. According to [6], a threshold chloride content exists for each cement, depending on the alkali, C_3A and aluminoferrrite content (of the cement). The cation of the chloride plays a role too: $CaCl_2$ is more dangerous from this point than NaCl. Although more chloride is bound in the former case but this is counteracted by a decreased OH^--concentration.

Further influences on chloride binding should also be taken into consideration, e.g. the sulfate content [7]. A competition occurs between sulfates and chlorides to react with C_3A (or aluminoferrite phases), and this is won by the sulfates, with a simultaneous increase of the Cl^--concentration in the pore solution. The cation of the sulfate plays a role, too: the chloride binding capacity of cement decreases rapidly with increasing sulfate contents derived from sodium sulfate and calcium sulfate; at the same sulfate content, however, cement pastes containing $CaSO_4$ have

a higher chloride binding capacity than those containing Na_2SO_4 [8].

2. Experimental

2.1. Raw Materials, Sample Preparation and Exposure

Three sets of aluminoferrites (corresponding to C_4AF, C_6AF_2 and C_6A_2F) were prepared (CEMKUT Ltd., Budapest) from calcium carbonate, alumina and iron(III)-oxide powders by pressing them into small cylinders and subjected to multiple firing (after regrinding) in an electric furnace in oxidizing atmosphere. Purity and stoichiometry of the aluminoferrites was controlled by XRD, using the data of TABIKH and WEHT [9] and TAMÁS and KOVÁCS [10]. Gypsum was pure natural gypsum rock, the same as used in cement factories. Three series of samples, (13 samples in each series) were prepared. *Table 1* shows sample and exposure variables.

Table 1. Samples and their exposure

Mass ratio of ferrite (C_4AF) to gypsum	Curing/exposure
10/0	100% r.h.
10/1	100% r.h.
10/2	100% r.h.
10/3	100% r.h.
10/4	100% r.h.
10/5	100% r.h.
10/1	100% r.h. + salt curing
10/2	100% r.h. + salt curing
10/3	100% r.h. + salt curing
10/4	100% r.h. + salt curing
10/5	100% r.h. + salt curing
10/3	Steam curing + 100% r.h.
10/3	Steam curing + salt curing

The materials were finely ground to pass sieve 0.063 mm, mixed according to *Table 1*, water added to have similar workability, and cast into $10 \times 10 \times 50$ mm prisms. After 24 hrs prisms were removed, kept at room temperature ($22 \pm 3\,^{\circ}C$), 100% r.h. Steam-curing was done for 6 hrs, $70\,^{\circ}C$, followed by a similar treatment as non-steamed ones. Salt treatment means to keep samples in 10% NaCl solution,

between the 28th and 56th days (24 hrs in the salt solution, followed by 24 hrs of drying); after this time salt-treated samples were kept at room temperature, 100% r.h.

Examination of hardened samples was done after 24 hrs, 28, 56, 90 and 180 days.

2.2. Methods of Investigation

The main method of investigation (all samples, at all ages) were thermal tests (TG/DTG/DTA) using the Derivatograph 1500-Q. In most cases the DTG curve proved to be adequate, as all peaks are endothermal, thus DTA did not give surplus information as contrasted to the more sensitive DTG curve. Data of thermal tests: inert material - alumina, heating rate $-10\,^{\circ}$C/min, up to 980 °C, in air atmosphere. Evaluation was computer-controlled. Tables give weight losses (in per cent of the original weight of the sample). As a secondary method, XRD was used, with CuK_{α} radiation.

Lack of space does not permit to present all data, thus only sample DTG curves or XRD patterns are shown. Details can be retrieved via the corresponding author.

2.3. Hydration of C_4AF

2.3.1. Hydration of C_4AF in Water

If water reacts with C_4AF, similar phases are formed as in case of C_3A hydration: hexagonal hydrates, which are later transformed into the stable phase, cubic hydrogarnet, $C_3/AF/H_6$. Three peaks are seen in the DTG-curve of the no-gypsum sample, hydrated for 24 hrs: at 100, 170 and 280 °C, corresponding to moisture, hexagonal hydrates and hydrogarnet, resp. This latter loses the remaining 1 mol of crystal water at 450 °C. (*Fig. 1*).

A ‘shoulder’ at approx. 250 °C indicates the presence of hydrated iron oxide or alumina. The metal ion of these hydrated phases is not clear (even Mössbauer spectrometry did not give decisive results, some researchers [11] find the presence of $Fe(OH)_3$, while others [12], [13] that of $Al(OH)_3$ are more probable. The hexagonal hydrates $\rightarrow$ cubic hydrates transformation is slower in case of C_4AF than in case of C_3A.

Care must be taken when studying the hydration of C_4AF, as several factors may influence this reaction, e.g. even the mass of the reactants. Hydration is strongly exothermal, and the rate of hydration is temperature-dependent to a high extent, thus a higher mass of the solid may cause a local increase of temperature.

After 28 days of hydration, DTG curves are qualitatively similar, but intensities changed. The process of hydration is well seen by the increased water loss,

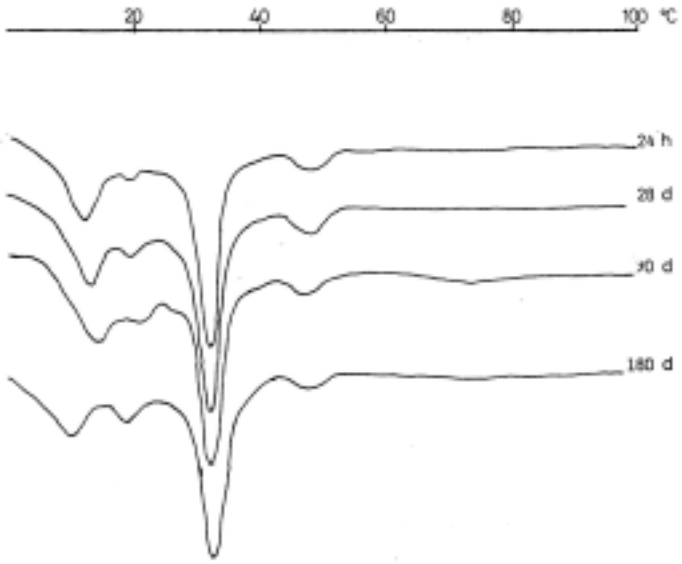

Fig. 1. DTG curves of hydrated C_4AF (sample 10/0), after 1, 28, 90 and 180 days of curing

corresponding to the hydrogarnet phase (from 8.4 to 12.0%). The peak is uniform, without sub-peaks, showing that a solid solution of C_3AH_6 and C_3FH_6 is formed.

2.3.2. Hydration of C_4AF + Gypsum Mixtures

The following phases can be detected in gypsum-containing samples besides the raw materials (C_4AF, gypsum): hexagonal hydrates ($C_2/AF/H_8$ or $C_4/AF/H_{13}$), cubic hydrate ($C_3/AH/_6$), ettringite (calcium-trisulfo-aluminate, $C_4/AF/\hat{S}_3H_{32}$), monosulfate (calcium-monosulfo-aluminate, $C_4/AF/\hat{S}H_{12}$), iron and/or aluminum hydroxide, as well as carbonates.

In the sample C_4AF, with gypsum in 10/1 mass ratio, after 24 hrs of hydration the DTG curve shows two intensive peaks, at approx. 100 and 174 °C. The former one can be attributed to the loss of moisture, but a part of ettringite crystal water is lost at the same temperature; this loss begins at approx. 50 °C, but continues later, with a maximum rate at 140 °C, while the one at 174 °C shows the presence of $C_4/AF/H_{13}$, but with two 'shoulders' at 140 °C and 190 °C; these are characteristic to the presence of ettringite and monosulfate, resp. The peak at 700 °C corresponds to the decarbonisation of calcium carbonate, formed by airborne CO_2. An upward bend of the DTG curve between 230 and 400 °C means weight loss, but cannot be assigned to one phase, as $C_4/AF/H_{13}$, hydrogarnet, ettringite and monosulfate lose water in this interval (*Fig. 2*).

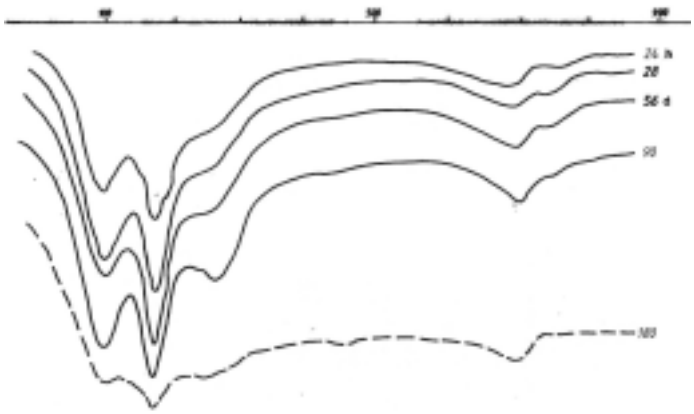

Fig. 2. DTG curves of hydrated C_4AF/gypsum (sample 10/1), after 1, 28, 90 and 180 days of curing

After 28 days, the most intensive peak of the DTG curve can be seen at 180 °C, but without the 'shoulders', indicating that the ettringite → monosulfate transformation is almost finished by this time.

After 56 days, only a slight change can be seen in the interval of 230–400°C: the one at 230 °C can be attributed to alumina or iron hydroxide (or both), while the one at 280 °C is due to the hydrogarnet phase, as the same one, with an increased intensity is visible in the sample hydrated for 90 days, jointly with the 450°C peak. The most marked difference is the increase of the intensity of the 280°C peak. No essential quantitative changes can be seen in the 180 days old sample, if contrasted to the 90 days one.

Results show that main hydration products of the 10/1 mixture of C_4AF and gypsum are $C_3/AF/H_6$, $C_4/AF/H_{13}$, $C_3/AF/C\hat{S}H_{12}$ and hydrated alumina or iron oxide, or both.

Sample series 10/2 mixture of C_4AF and gypsum contains after 24 hrs of hydration ettringite, $C_4/AF/H_{13}$ and monosulfate, by DTG peaks at 140, 160 and 185 °C, as well as hydrogarnet, $C_3/AF/H_6$, by DTG peak 270 °C. The 185 °C peak is very intensive, still it does not merge with the $C_4/AF/H_{13}$ peak, 20–25 °C lower, showing that there exists a miscibility gap between these two complexes. No ettringite is found in older samples; and AFm products are increasing. Moisture (100 °C) and calcium carbonate (700 °C) are present in all samples (*Fig. 3*).

Sample series 10/3 mixture of C_4AF and gypsum contains after 24 hrs of hydration gypsum, ettringite, $C_4/AF/H_{13}$ and monosulfate, by DTG peaks at 140, 155 and 175 °C; hydrogarnet (270 °C) content is much lower than in the 10/1 or 10/2 series at the same age. In older ages $C_4/AF/H_{13}$, and monosulfate as well as hydrogarnet peaks become more intensive; a small amount of ettringite (shoulder

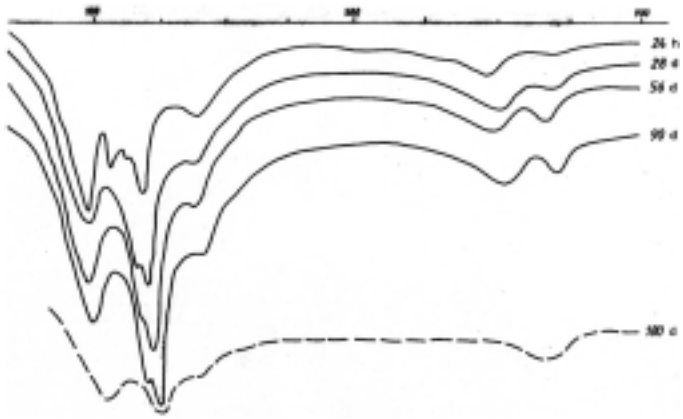

Fig. 3. DTG curves of hydrated C_4AF/gypsum (sample 10/2), after 1, 28, 90 and 180 days of curing

at 140 °C) persists in the 28-day sample, but it is absent later. Monosulfate peaks are more intensive than those of $C_4/AF/H_{13}$ at all ages. Main hydration products of series 10/3 are $C_3/AF/H_6$, $C_4/AF/H_{13}$ and $C_4/AF/\hat{S}H_{12}$ (*Fig. 4*).

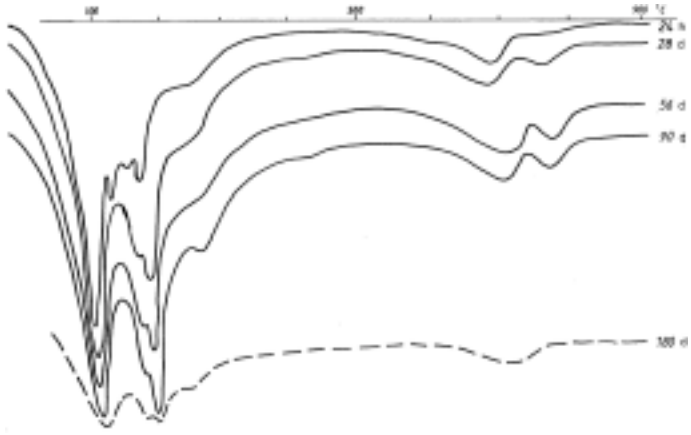

Fig. 4. DTG curves of hydrated C_4AF/gypsum (sample 10/3), after 1, 28, 90 and 180 days of curing

In series 10/4 an intensive DTG peak can be seen after 24 hrs, between 20–

137 °C, showing the presence of gypsum (double minima at 120 and 135°C). All other products of hydration give shoulders rather than peaks. After 28 days the 164 °C peak ($C_4/AF/H_{13}$) is more intensive than that of the 182 °C one (monosulfate), while in case of the older samples this order of intensity is inverted. The process of hydration can be seen by the increase of structural water content by 1–2% (*Fig. 5*).

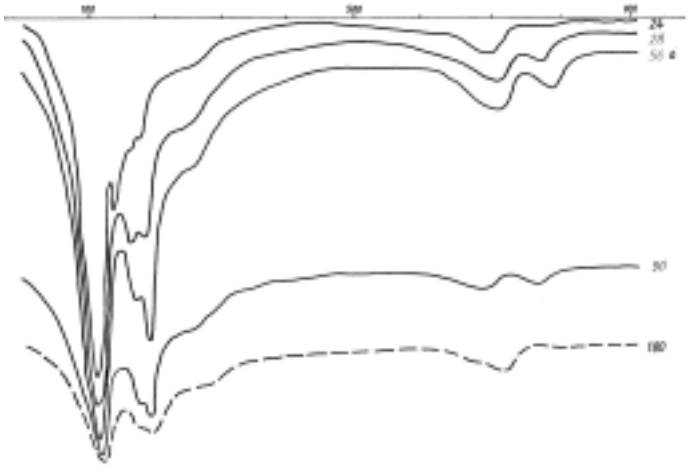

Fig. 5. DTG curves of hydrated C_4AF/gypsum (sample 10/4), after 1, 28, 90 and 180 days of curing

DTG curves of series 10/5 are qualitatively similar to the former one. Low temperature (< 120 °C) peaks are very intensive because of the presence of unreacted gypsum. Several references exist [1], [3], [14], [15] which claim that monosulfate is formed only after the exhaustion of gypsum by ettringite formation. In case of high gypsum content (with the exception of the 24 hr age) the $C_4/AF/H_{13}$ peak (170 °C) is always more intensive than that of the monosulfate peak (190°C). Gypsum is present even after 180 days of 100% r.h. exposure (*Fig. 6*).

2.3.3. Chloride Binding Capacity of C_4AF after NaCl Exposure

It is a well established fact, that C_4AF binds chlorides similarly to C_3A, by the formation of Friedel's salt $C_3A \cdot CaCl_2 \cdot H_{10}$, or its iron analogue $C_3F \cdot CaCl_2 \cdot H_{10}$, if chlorides are dissolved in the mixing water; hardly any data exist on hydrated C_3A or C_4AF exposed to chloride-containing water [5]. The question gets still more complicated in case of hardened cement paste, and esp. in case of concrete, where other clinker minerals, admixtures, additives, aggregates all influence the nature of the hydration product. To clear these questions, a series of salt-treated samples was

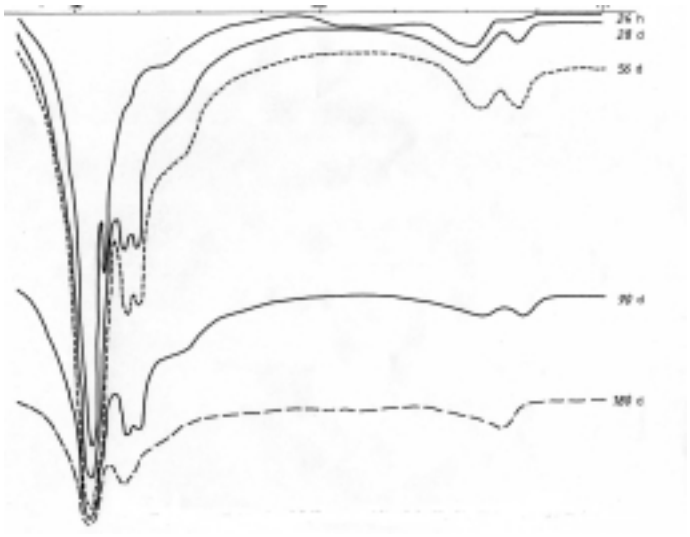

Fig. 6. DTG curves of hydrated C_4AF/gypsum (sample 10/5), after 1, 28, 90 and 180 days of curing

prepared: C_4AF – gypsum mixtures 10/1, 10/2, 10/3, 10/4 and 10/5 were hydrated in water for 28 days, and the hardened samples exposed 10% NaCl solution for one day, followed by 1 day of drying. This process was done from the 28-th to the 56-th day. After this time the samples were kept in a 100% r.h. cabinet, as described in par. 2.1.

The most striking difference, as contrasted to non-salt-treated samples is the presence of a flat, but well recognizable peak at approx. 310 °C, which can be attributed to Friedel's salt, its iron analogue $C_3F \cdot CaCl_2 \cdot 10H_2O$, or their solid solution. About 40% of the water content of this phase is lost at 120–130 °C. Other indications show that the chloro-aluminate ferrite AFm phase may form solid solutions with other, sulfate-containing AFm phases or with $C_4/AF/H_{13}$.

Another interesting feature of the salt-treated samples is that the two high-temperature peaks, caused by decarbonisation (690 and 770 °C) are not present; on the other hand, a new peak, well distinguishable from former ones appears at 710 °C. The loss of the CO_2 peak is probably that the carbonate ion is incorporated into the AFm phases as hemi-, or monocarbo-aluminate; the new peak is due to the sublimation of NaCl from the surface of the sample. An interesting consequence of carbo-aluminate formation is the formation of secondary ettringite, as observed by [16], [17]. They conclude that at high pH values (> 12) the monosulfate is unstable in the presence of CO_2, and the sulfate can be replaced by the carbonate group, causing the formation of $C_3A \cdot CaCO_3 \cdot H_{11}$; this increases the sulfate-ion concentration of the solution and thus helps ettringite formation.

When comparing the DTG curves of salt-treated and non-salt-treated samples, at identical gypsum levels, no striking differences can be seen in younger (1-day and 28-day) samples; in older samples, on the other hand, a new peak of 310 °C appears, near to the 260–270 °C one. This is caused by Friedel's salt, or its iron-containing analogue. Another interesting feature mentioned previously is that one peak appears (at 710 °C), replacing the double peak of carbonates. The peak caused by AFm phases at approx. 180 °C shows a single peak in salt-treated, rather than the double one (170 and 190 °C) in non-salt-treated samples.

A next series was investigated to disclose the effect of steam-cured samples, both non-salt-treated and salt-treated ones. In this series only the 10/3 C_4AF/gypsum sample was investigated. The main difference: AFm phases give a single peak at $\sim$ 190 °C. In case of steam-cured samples the two end-products of hydration, i.e. $C_3/AF/H_6$ and monosulfate are present even after 24 hrs. It looks like that in the presence of gypsum the first step of hydration is the formation of ettringite; but steam-curing causes a rapid transformation of $C_4/AF/H_{13}$ to $C_3/AF/H_6$; as a gross effect, monosulfate and $C_3/AF/H_6$ are formed practically simultaneously.

It is a difficult task to calculate phase percentages using thermal analysis; the TG curve, even with the aid of DTG does not give exact information, not even when DTG peaks are well separated, as not only starting compounds react, but also newly formed ones, with themselves or with original ones. In our study the Friedel's salt phase was approximately calculated by measuring the mass decrease between 290 and 330 °C of salt-treated samples, compared to similar, but non-salt-treated ones (*Table 2*).

Table 2. Quantity of $C_3/AF/CaCl_2 \cdot H_{10}$, per cent, in salt-treated C_4AF

C_4AF/gypsum	After 56 days	After 90 days	After 180 days	Average
10/1	–	–	–	–
10/2	7.7	7.7	–	7.7
10/3	–	–	15.3	15.3
10/4	–	–	–	–
10/5	–	22.9	23.0	23.0
10/3, steam-cured	–	9.6	9.6	9.6

2.3.4. Conclusions of Thermal Testing

1. The presence of calcium aluminate/ferrite-chloro-hydrate AFm phase, $C_3/AF/ \cdot CaCl_2 \cdot H_{10}$ was established, by its DTG peak between 290–315 °C, in all salt-treated specimens, independently of the gypsum content. *Fig. 7* compares non-salt-treated and salt-treated DTG curves of 56 days old, 10/1, 10/3 and 10/5 samples. Main differences in salt-treated samples:

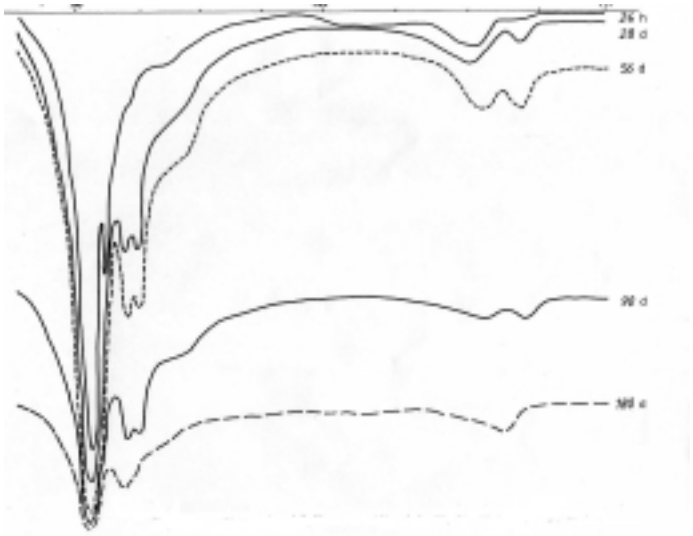

Fig. 7. Comparison of DTG curves of hydrated, and hydrated/salt-treated C_4AF/gypsum (samples 10/1, 10/3 and 10/5), after 56 days of curing

- Appearance of the $C_3/AF/\cdot CaCl_2\cdot H_{10}$ peak at $\sim$ 310 °C
- Broadening of the AFm peak (from 150–210 °C to 130–210 °C)
- Disappearance of the two carbonate peaks (670 and 740 °C); a single peak appears instead, at $\sim$ 710 °C, due to NaCl sublimation.

It should be mentioned, however, that in case of non-salt-treated samples the monosulfate peak (190 °C) is more intensive, than that of the $C_4/AF/H_{13}$ (170 °C) in the 10/3 mixture, while the intensity order is inverted in the 10/5 mixture. This shows that the metastable calcium-aluminate-ferrite hydrate is more easily transformed into Friedel's salt (or its iron analogue) than the monosulfate phase. This is why the most intensive 310 °C peak appears at the 10/5 sample.

2. It cannot be established if Friedel's salt, or its iron analogue or their solid solution are present, as they have identical crystal structures and thus thermal peaks (and also X-ray patterns) are similar.

3. All AFm phases ($C_4/AF/H_{13}$, monosulfate, iron monosulfate, Friedel's salt, iron Friedel's salt or even $C_3/AF/\cdot CaCO_3\cdot H_{10}$) may form solid solutions, but usually a miscibility gap exists between them. This is why the DTG peak at $\sim$ 160–200 °C is sometimes single, and sometimes divided to partial minima.

2.3.5. Additional Results of C_4AF Hydration by XRD

X-ray diffraction was used as an additional method to characterize all samples; although thermal tests enable a quantitative characterization, but in multicomponent systems, if several compounds give a DTA/DTG peak in the same temperature interval, phase identification is not always possible. XRD can qualitatively help in such cases, using a computer comparison of known XRD patterns with our own spectra [18]. It should be mentioned that all results of the former paragraphs have been corroborated by XRD results.

Only some samples of XRD-pattern are shown in this paper. The steam-cured sample 10/3 after 28 days shows intensive peaks of monosulfate ($C_4/AF/\hat{S}H_{12}$), ettringite ($C_6/AF/\hat{S}_3H_{31}$) and those of unhydrated C_4AF. Low-intensity peaks indicate the presence of small quantities of $C_3/AF/H_6$ and gypsum (*Fig. 8*). In the same material, after NaCl curing the pattern shows the presence of the chloride-containing AFm phase, $C_3/AF/\cdot CaCl_2 \cdot H_{10}$ too, while gypsum is not present any more.

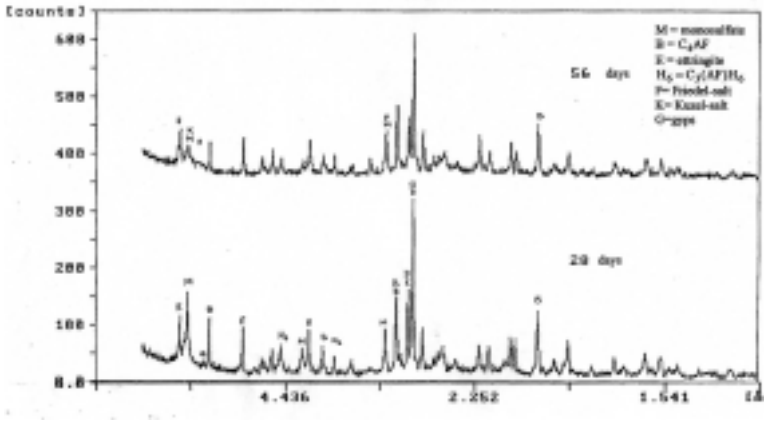

Fig. 8. X-ray diffraction patterns of steam-cured C_4AF/gypsum (sample 10/3), age 28 days and that of steam-cured and salt-treated C_4AF/gypsum (sample 10/3), age 56 days

Although XRD was used as an additional method only, still it can give interesting informations. On the DTG curve of steam-cured sample 10/3 and the same, but salt-treated one, age of 56 days the AFm peaks are of similar intensity; still their XRD patterns are different: in the non-salt-treated sample. In the non-salt-treated sample monosulfate reflections are intensive, while in the salt-treated, but otherwise similar sample these peaks are faint. Reflections of Friedel's salt are also weak, but among the low-intensity peaks between 7.8–9.6 Å lattice spacings a new peak can be seen, at 8.51 Å. This peak can be assigned to Kuzel's salt [17], $C_3/AF/\cdot 1/2CaSO_4 \cdot 1/2CaCl_2 \cdot H_{11}$. A solid solubility of Friedel's salt, Kuzel's

salt and other AFm phases exists, but with certain gaps. Friedel's salt stabilizes the monosulfate phase by the formation of Kuzel's salt.

Unfortunately neither thermal tests, nor XRD can differentiate between C_3AH_6, C_3FH_6, and their solid solution $C_3/AF/H_6$, and similarly between $C_3A \cdot CaCl_2 \cdot H_{10}$, $C_3F \cdot CaCl_2 \cdot H_{10}$, and their solid solution $C_3/AF/ \cdot CaCl_2H_{10}$. XRD, on the other hand, gives surplus information on the presence of ettringite: small XRD peaks of ettringite are seen even if the DTG curve shows no peaks. In the 10/2 mixture, after 56 days of hydration gypsum XRD peaks are still visible, jointly with strong monosulfate peaks.The theory, which claims that monosulfate occurs only after the total exhaustion of gypsum, is false.

3. Summary and Conclusions

1. Hydration products of C_4AF are similar to those of C_3A, only alumina is partly or fully replaced by iron oxide. The transformation rate of metastable iron-containing calcium-aluminate-ferrite-hydrates ($C_4/AF/H_{13}$, $C_2/AF/H_8$), to the stable hydrogarnet phase, however, is slower, than in case of iron-free compounds (although $C_3/AF/H_6$ is present even after one day of hydration). C_3AH_6, C_3FH_6 or their solid solution $C_3/AF/H_6$ cannot be distinguished by the methods (thermal analysis, XRD) used in this study.
2. Hydration products of C_4AF + gypsum mixtures are, besides those mentioned under 1. 'monosulfate' ($C_3/AF/ \cdot CaSO_4 \cdot H_{12}$) and ettringite ($C_3/AF/ \cdot 3CaSO_4 \cdot H_{31}$). Monosulfate was found, in contrary to [1], prior to the total exhaustion of gypsum. Ettringite, in some cases was not detectable by thermal tests, due to its low quantity but it was seen in low-intensity peaks on XRD patterns. Metastable hexagonal hydrates, of general formula $[Ca_2/Al, Fe/(OH)_6]OH \cdot xH_2O$ were detected by thermal tests in each of the non-steam-cured samples.
3. In all salt-cured C_4AF/gypsum mixtures the iron-containing AFm phase, Friedel's salt ($C_3/AF/ \cdot CaCl_2, H_{10}$) was detected, by thermal as well as XRD tests, independently of the gypsum quantity.
4. The AFm phases $C_4/AF/H_{13}$, $C_4/AF/\hat{S}H_{12}$, $C_4/AF/ \cdot CaCl_2 \cdot H_{12}$, $C_4/AF/ /\hat{C}H_{12}$ may form solid solutions; this series is not continuous. This explains the fact that the DTG peak of the AFm peak is sometimes single, and sometimes divided by a transient maximum. After salt-treatment, however, AFm phases show a single minimum on the DTG curve.
5. Less Cl^- was bound in steam-cured ferrite phases than in similar, but non-salt-treated samples.

Table 3. C_4AF Mass Losses by TGA (initial sample mass = 100)

Age	24 hrs				28 days				Age: 56 days				
Temp. interval	130–600 °C	20–130 °C	600–900 °C	20–900 °C	130–600 °C	20–130 °C	600–900 °C	20–900 °C	130–600 °C	20–130 °C	600–900 °C		20–900 °C
Mass loss %	Structural H_2O	Moisture	CO_2	Σ	Structural H_2O	Moisture	CO_2	Σ	Structural H_2O	Moisture	CO_2	CO_2 and/or NaCl	Σ
10/1	8.33	4.20	2.19	14.72	12.43	5.83	1.71	19.97	12.87	5.70	3.18	–	21.75
10/2	8.00	4.18	1.70	13.88	11.62	4.50	3.11	19.23	12.36	6.45	2.84	–	21.65
10/3	8.22	6.46	2.15	16.83	11.27	8.43	2.56	22.26	11.83	7.65	3.01	–	22.49
10/4	8.07	7.81	2.04	17.92	10.61	9.93	2.69	23.23	11.24	10.28	3.50	–	25.02
10/5	7.82	8.48	1.93	18.23	9.22	13.28	4.10	26.60	12.32	12.73	2.36	–	27.42
10/1*	9.09	5.57	1.55	16.21	12.39	4.07	2.70	19.16	13.79	6.36	–	3.16	23.31
10/2*	9.39	4.28	1.97	15.64	12.83	5.73	2.40	20.96	13.03	4.93	–	2.40	20.36
10/3*	9.11	3.96	1.69	14.76	12.03	7.95	1.85	21.83	11.83	7.75	–	2.54	22.12
10/4*	9.15	7.03	1.73	17.91	10.65	12.18	2.93	25.76	11.19	9.97	–	4.07	25.23
10/5*	7.82	9.24	1.83	18.89	10.47	14.09	1.51	26.07	12.17	12.05	–	4.10	28.32
10/3°	12.44	4.92	2.91	20.27	13.22	6.44	2.19	21.85	13.33	6.99	2.62	–	22.94
10/3^	12.28	4.92	2.29	19.49	12.81	5.55	1.90	20.26	13.46	6.58	–	2.63	22.67
10/0	8.42	5.42	1.18	15.02	12.01	4.70	1.48	18.19					

Age	90 days					180 days				
Temp. interval	130–600 °C	20–130 °C	600–900 °C		20–900 °C	130–600 °C	20–130 °C	600–900 °C		20–900 °C
Mass loss %	Structural H_2O	Moisture	CO_2	CO_2 and/or NaCl	Σ	Structural H_2O	Moisture	CO_2	CO_2 and/or NaCl	Σ
10/1	12.70	5.99	2.31	–	21.00	14.00	4.40	3.80		22.20
10/2	13.07	6.26	3.10	–	22.43	13.52	5.60	4.10		23.22
10/3	12.06	8.65	2.81	–	23.52	13.00	7.90	3.30		24.20
10/4	13.59	10.53	2.36	–	26.48	13.99	9.91	3.40		27.30
10/5	13.89	12.09	2.84	–	28.82	13.80	12.30	3.90		30.00
10/1*	13.68	5.77	–	2.35	21.80	13.67	7.41		2.96	24.00
10/2*	12.86	5.98	–	2.16	20.90	12.43	5.36		3.02	20.80
10/3*	12.45	7.51	–	2.35	22.31	12.91	7.04		3.22	23.17
10/4*	13.02	11.30	–	4.19	28.51	13.53	8.04		4.45	26.02
10/5*	12.43	14.55	–	3.84	30.73	12.93	11.50		4.01	28.44
10/3°	13.36	6.55	2.82	–	22.73	13.43	5.92	3.52		22.87
10/3^	13.17	6.30	–	2.90	22.37	13.52	6.08		2.87	22.47

No symbol: 100% r.h.
*: 100% r.h. + salt treatment
°: steam curing + 100% r.h.
^: steam curing + salt treatment

Acknowledgements

This research was supported by the Hungarian National Scientific Research Foundation (OTKA), Grant No. T019414. Authors are grateful for funding and continuous support of OTKA.

Ferrite material (C_4AF, C_6A_2F, C_6AF_2) was provided by CEMKUT Ltd. (Budapest) and personally by Dr. M. Révay. XRD investigations were done at the Department of Mineralogy, Technical University of Budapest. Authors are indebted to Mrs. K. Kopecsko-Kocsányi for XRD investigations, and to Mrs. E. Felszeghy for DTG tests.

References

[1] COLLEPARDI, M – MONOSI, S. – MORICONI, G. – CORRADI, M: Tetracalcium-aluminoferrite Hydration in the Presence of Lime and Gypsum, *Cem. Concr. Res.* **9** (4) (1979) pp. 431–437.
[2] EMANUELSON, A. – HANSEN, S.: Distribution of Iron Among Ferrite Hydrates, *Cem. Concr. Res.* **27** (8) (1997) pp. 1167–1177.
[3] SURYAVANSHI, A. K. – SCANTLEBURY, J. D. – LYON, S. B.: The Binding of Chloride Ions by Sulphate Resistant Portland Cement, *Cem. Concr. Res.* **25** (3) (1995) pp. 581–592.
[4] BIRNIN-YAURI, U. A. – GLASSER, F. P.: Friedel's Salt, $Ca_2Al(OH)_6(Cl,OH) \cdot 2H_2O$: Its Solid Solutions and Their Role in Chloride Binding, *Cem. Concr. Res.* **28** (12) (1998) pp. 1713–1724.
[5] SURYAVANSHI, A. K. – NARAYAN SWAMY, R.: Stability of Friedel's Salt in Carbonated Concrete Structural Elements, *Cem. Concr. Res.* **26** (5) (1996) pp. 729–742.
[6] RASHEEDUZZAFAR, ENTESHAM HUSSAIN, S. – AL-SADOOM, S. S.: Effect of Cement Composition on Chloride Bonding and Corrosion of Reinforcing Steel in Concrete, *Cem. Concr. Res.* **21** (5) (1991) pp. 777–794.
[7] ENTESHAM HUSSAIN, RASHEEDUZZAFAR, S. – AL-GAHTANI, A. S.: Influence of Sulfates on Chloride Binding in Cements, *Cem. Concr. Res.* **24** (1) (1994) pp. 8–24.
[8] XU, Y.: Influence of Sulfates on Chloride Binding and Pore Solution Chemistry, *Cem. Concr. Res.* **27** (12) pp. 1841–1850.
[9] TABIKH, A. A. – WEHT, R. J.: An XRD Analysis of Portland Cement, *Cem. Concr. Res.* **1** (3) (1971) pp. 317–328.
[10] TAMÁS, F. D. – KOVÁCS, K.: A Generalization and Computer Solution of the Bogue Calculation, *Cement Technology*, **5** (4) (1974) pp. 393–401.
[11] FORTUNE, J. M. – COEY, J. M. D.: Hydration Products of Calcium Aluminoferrite, *Cem. Concr. Res.* **13** (5) (1983) pp. 696–702.
[12] TAMÁS, F. D. – VÉRTES, A.: Brownmillerite Hydration by Mössbauer Spectrometry, *Hung. J. Industrial Chem.* **3** (3) (1975) pp. 337–385.
[13] HARCHAND, K. S. – KUMAR, R. – CHANDRA, K.: Vishwamittar, Mössbauer and X-ray Investigations on Some Portland Cements, *Cem. Concr. Res.* **14** (2) (1984) pp. 170–176.
[14] BALÁZS, GY. – CSIZMADIA, J. – KOVÁCS, K.: Chloride Ion Binding Ability of Calcium-Aluminate, -Ferrite and -Silicate Phases. *Periodica Polytechnica*, **41** (2) (1997) pp. 147–168.
[15] JAWED, I. – GOTO, S. – KONDO, R.: Hydration of Tetracalcium Aluminoferrite in the Presence of Lime and Sulfates, *Cem. Concr. Res.* **6** (3) (1976) pp. 441–454.
[16] GLASSER, F. P. – KINDNESS, A. – STRONACH, S. A.: Stability and Solubility Relations in Afm Phases, Part I. Chloride, Sulfate and Hydroxide, *Cem. Concr. Res.* **29** (6) (1999) pp. 861–866.
[17] KUZEL, H.-J. – PÖLLMANN, H.: Hydration of C_3A in the Presence of $Ca(OH)_2$, $CaSO_4 \cdot 2H_2O$ and $CaCO_3$.
[18] TAYLOR, H. F. W.: Cement Chemistry, Academic Press, New York, 1990.